

Magnetic Anisotropy in $\text{Co}^{\text{II}}\text{X}_4$ ($\text{X} = \text{O}, \text{S}, \text{Se}$) Single-Ion Magnets: Role of Structural Distortions versus Heavy Atom Effect

Arup Sarkar,^[a] Subrata Tewary,^[a, b] Shwetal Sinkar,^[a] and Gopalan Rajaraman^{*[a]}

Abstract: Mononuclear four coordinate Co^{II} complexes have drawn a great deal of attention as they often exhibit excellent single-ion magnet (SIM) properties. Among the reported complexes, the axial zero-field splitting parameter (D) was found to vary drastically both in terms of the sign as well as strength. There are various proposals in this respect such as structural distortions, heavier atom substitution, metal-ligand covalency, tuning secondary coordination sphere, etc. that are expected to control the D values. To assess the importance of structural distortions vs. heavier atom substitution effect, here we have undertaken detailed theoretical studies based on the ab initio CASSCF/NEVPT2 method to estimate zero-field splitting parameters for twelve complexes reported in the literature. Our test set includes the $\{\text{Co}^{\text{II}}\text{X}_4\}$ (where $\text{X} = \text{O}, \text{S}, \text{Se}$) core structure where the D value was found to vary from $+19$ to -118 cm^{-1} . Based on the structural variation, we have classified the complexes into three

types (I–III) where type I complexes were found to exhibit the largest negative D value as desired for SIMs. The other two types (II and III) of complexes have been found to be inferior with respect to type I. The secondary coordination sphere was also found to influence D , as substitution on the secondary coordination sphere atom was found to significantly alter the magnitude of D values. Particularly, two structural parameters, namely, the dihedral angle between the two ligand planes and the $\angle\text{X-Co-X}$ polar angle were found to heavily influence the sign and strength of D values. Our analysis clearly reveals that these structural factors are much more important than the heavier atom substitution, or metal-ligand covalency. A large variation in the D and E/D values among these complexes despite possessing a very close structural similarity offers an exquisite playground for a chemist to design and develop new-generation Co^{II} -based SIMs.

Introduction


Single molecule magnets (SMM) are a class of molecule based nanomagnets that considered to be a potential alternative to the high-dense information storage devices.^[1] Recently various Dy^{III} Single-ion Magnets (SIMs) based on cyclopentadienyl ligands have been reported to possess blocking temperature exceeding liquid nitrogen temperatures, bring the possibility of storing information in individual molecule closer to the reality.^[2] A good SIM is the one, which yields large barrier height for magnetisation reversal (U_{eff}) and this barrier height arises due to the magnetic anisotropy embedded in axial zero-field splitting parameter (D) of the associated M_S levels. In this regard, first-row mononuclear transition metal complexes con-


taining Fe, Co, Ni complexes were found to be promising as they show high blocking barrier in recent years.^[3] There are various challenges in obtaining very large U_{eff} values in transition metal ions based SIMs, (i) the sign of zero-field splitting which decide whether a largest M_S or smallest being the ground state has to be negative (ii) the magnitude of zero-field splitting should be ideally of the order of hundreds of wave-number (iii) as these are quantum systems, there are several other relaxation processes other than the regular Orbach mechanism wherein quantum tunnelling between the M_S (QTM) levels is of utmost important as this control the relaxation of magnetization at very low temperatures. To circumvent these problems, Co^{II} complexes are the most popular choice as it offers very large magnetic anisotropy whose sign can be modulated using the ligand field. Additionally, as it has Kramers ground state, formally the QTM is forbidden and hence offer attractive blocking temperatures. Moreover, the coordination number around the Co^{II} ion can be modulated to enhance the anisotropy which will eventually lead to very large U_{eff} values as seen recently in a two-coordinate Co^{II} SIMs.^[3c,d]

Despite the fact that the two coordinate Co^{II} complexes exhibit very large U_{eff} values, these complexes are not air-stable and hence are difficult to subject them for fabricating devices.^[4] Most robust complexes based on Co^{II} belong to four coordinate tetrahedral geometries where various means are proposing to fine tune both the sign and magnitude of the zero-field splitting parameter. While $\{\text{CoS}_4\}$ remains one of the thoroughly studied systems and exhibit U_{eff} values as large as

[a] A. Sarkar, S. Tewary, S. Sinkar, Prof. G. Rajaraman
Department of Chemistry
Indian Institute of Technology Bombay
Powai, Mumbai 400076 (India)
E-mail: rajaraman@chem.iitb.ac.in

[b] S. Tewary
Current address: RIKEN Center for Computational Science
7-1-26, Minatojima-minami-machi, Chuo-ku, Kobe, 650-0047 (Japan)

 Supporting information and the ORCID identification number(s) for the author(s) of this article can be found under:
<https://doi.org/10.1002/asia.201901140>.

 This manuscript is part of a special issue celebrating the 20th anniversary of the Chemical Research Society of India (CRSI). Click here to see the Table of Contents of the special issue.

62 cm^{-1} ,^[5] how the magnitude and the sign of D values vary if mixed donor ligands are employed has not been explored in detail.

Ab initio calculations are proven to a powerful tool in this area wherein methodology based on multi-reference CASSCF/NEVPT2 methods have been utilized to compute zero-field splitting parameters of various transition metal SIMs successfully.^[6] Particularly in tetrahedral Co^{II} complexes, this methodology has been used to even predict suitable target molecules possessing very large negative D values.^[5,7] Here in this manuscript, we attempt to undertake a theoretical study based on ab initio CASSCF methods to understand and predict the anisotropy in twelve Co^{II} complexes containing $[\text{CoX}_4]$ ($X=\text{O}, \text{S}$ and Se) cores which are reported in the literature. The complexes are chosen in such a way that we could address one of the perennial problems in understanding the magnetic anisotropy in tetrahedral Co^{II} complexes.

Particularly the heavier atom effects and its role in influencing the magnitude and sometimes even sign is highlighted^[8] and this lead to several proposals that such substitutions are the way forward to obtain large negative D values. On the other hand, several such heavier atom containing tetrahedral Co^{II} found to possess small and positive D values, suggesting clearly that there are various factors at play and a vanilla recipe for obtaining large negative D unlikely to yield the desired results. To systematically understand the nature of magnetic anisotropy and also to develop magneto-structural maps that are correlated to the D parameters, herein we have studied twelve such complexes that possess a variety of coordination sites and differ in terms of ligand substitutions. The molecular formula of the twelve complexes that are studied here are as follows- $[\text{Co}^{\text{II}}\{\text{N}(\text{OPPh}_2)(\text{SPPH}_2)\text{-O,S}\}_2]$ (CCDC 641241) (1),^[9] $[\text{Co}\{\text{PhC}(\text{S})\text{-N-P}(\text{O})(\text{O}i\text{Pr})_2\}_2]$ (CCDC 225507) (2),^[10] $[\text{Co}\{\text{PhNHC}(\text{S})\text{-N-P}(\text{O})(\text{OPr-}i)_2\text{-O,S}\}_2]$ (CCDC 606359) (3),^[11] $[\text{Co}\{i\text{PrNHC}(\text{S})\text{-N-P}(\text{O})(\text{O}i\text{Pr})_2\}_2]$ (CCDC 621219) (4),^[12] $[\text{Co}\{\text{N}(\text{SOCN}i\text{Pr}_2)_2\}_2]$ (CCDC 715970) (5),^[13] $[\text{Co}\{\text{Ph}_2\text{P}(\text{Se})\text{NP}(\text{Se})\text{Ph}_2\}_2]$ (CCDC 137590) (6),^[14] $[\text{Co}\{\text{Ph}_2\text{PSNPSPh}_2\}_2]$ (CCDC 139529) (7),^[15] $[\text{Co}\{\text{N}(\text{SePiPr}_2)_2\}_2]$ (CCDC 102141) (8),^[16] $[\text{Co}\{\text{N}(\text{SPiPr}_2)_2\}_2]$ (CCDC 102143) (9),^[16] $[\text{Co}\{\text{Ph}_2\text{PSCHPSPH}_2\}_2]$ (CCDC 812004) (10),^[17]

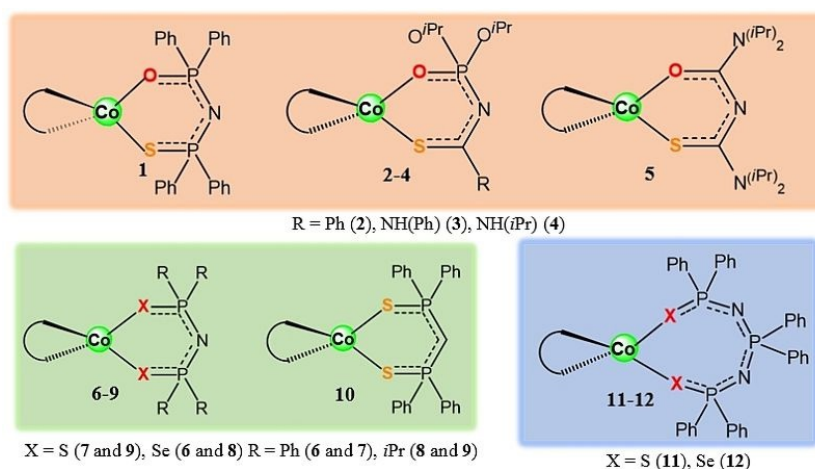
$[\text{Co}\{\text{SPh}_2\text{PNPPH}_2\text{NPPH}_2\text{S}\}_2]$ (CCDC 1235748) (11),^[18] $[\text{Co}\{\text{SePh}_2\text{-PNPPH}_2\text{NPPH}_2\text{Se}\}_2]$ (CCDC 1235750) (12).^[18] The structures are chosen in such a way that both the donor atoms as well as the atoms in the secondary coordination sphere vary to assess the sign and strength of ZFS parameters. For example, the donor atoms in this list contain, O, S and Se bidentate ligands where the secondary coordination sphere contain N, C or P offering rigid ligand framework around the metal centre. A schematic diagram depicting complexes 1–12 is given in Scheme 1 and their X-ray structures along with the computed direction of D_{zz} axis are shown in Figure 1.

Computational Methodology

Ab initio calculations were performed with CASSCF/NEVPT2 methodology as implemented in ORCA 4.0.1 program package.^[19] All the calculations were performed on the crystal structures reported. Scalar relativistic Hamiltonian was considered by using ZORA (zeroth-order regular approximation) method.^[20] Also, ZORA contracted versions of basis sets ZORA-def2-TZVP were used for Co, S, Se; ZORA-def2-TZVP(-f) for N and O; and ZORA-def2-SVP were used for rest of the atoms throughout the calculations.^[21] SA-CASSCF (State-average complete active space self-consistent field) calculations were carried out within an active space of seven electrons in five 3d-orbitals, i.e., CAS(7,5) and the orbitals are optimised with 10 quartets and 40 doublet roots. The NEVPT2 (N-electron valence perturbation theory 2nd order) part of the calculation incorporates the dynamic correlation into account. Spin-orbit coupling was treated with spin-orbit mean field (SOMF) operator, and subsequent spin state mixing was obtained with QDPT (quasi-degenerate perturbation theory) method. Final Spin-Hamiltonian properties were computed with universal EHA (effective Hamiltonian approach) method.^[22]

Results and Discussion

We have classified the twelve complexes into three types based on structural distortions present in their first coordina-



Scheme 1. Two dimensional structural representation of complexes 1–12 based on X-ray geometries. The ligands are symmetric around the Co^{II} centre. The substitution groups include, Ph = Phenyl, *i*Pr = isopropyl and. Type I- orange box, type II- green box and type III- blue box.

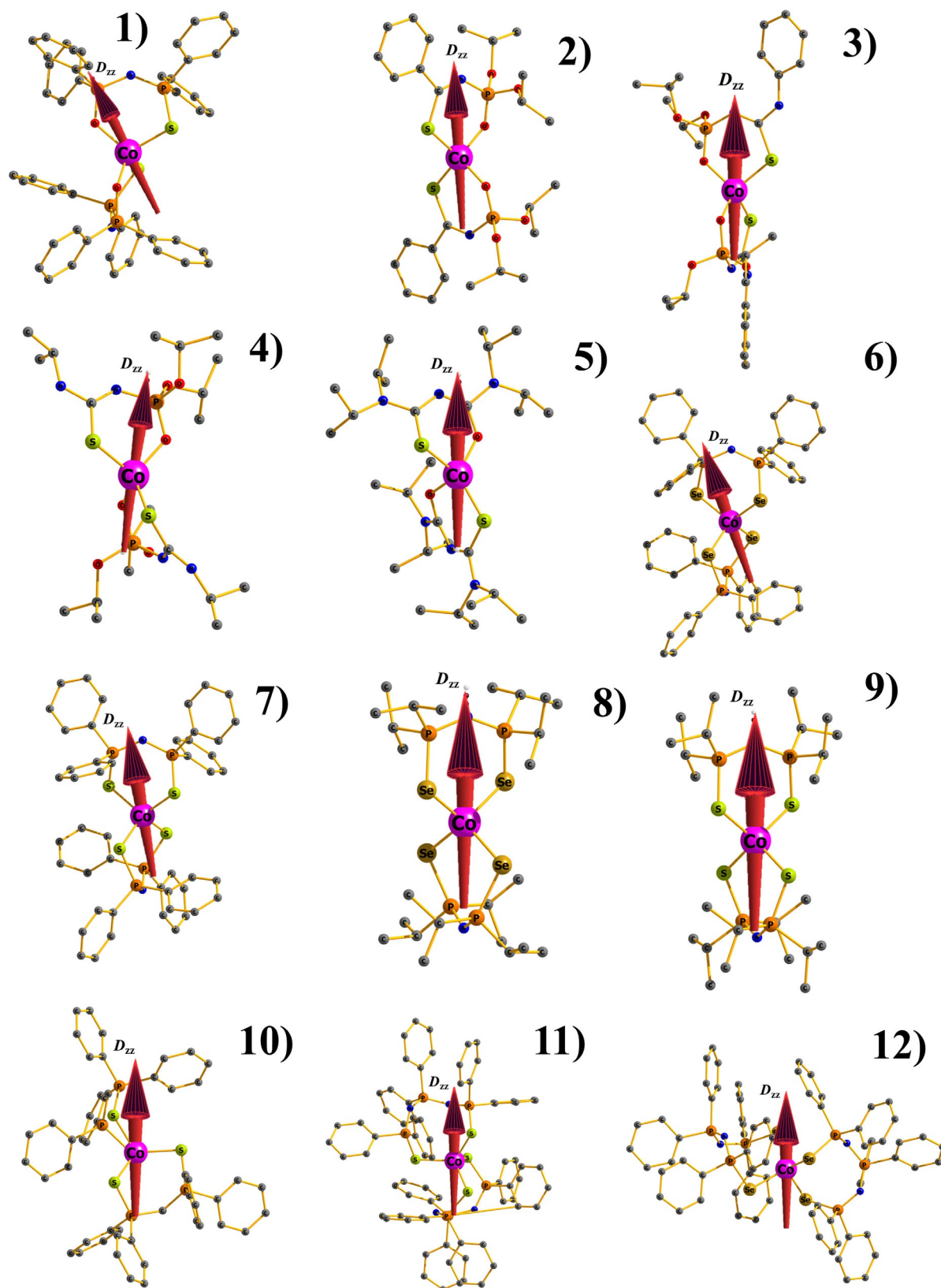


Figure 1. Ball and stick representation of X-ray structures along with computed D_{zz} orientations for all the complexes. Hydrogen atoms were removed for clarity. Colour code: Grey=C; Blue=N; Red=O; Orange=P; Yellowish green=S; Golden yellow=Se.

tion sphere: type / comprises complexes which have $\{CoO_2S_2\}$ core and the complexes 1–5 belong to this category. The dif-

ference among 1–5 arises in the substituents present in the chelate ring at the phosphorous/carbon centres from the

second coordination sphere (Scheme 1). The substitution at the phosphorous atom includes -phenyl, *N*-(di-isopropoxy) and *O*-(di-isopropoxy) groups whereas the substituted groups at the carbon centre are -phenyl, -phenyl amine and -isopropyl amine groups. The type *II* set comprise complexes 6–10 which have {CoX₄} core (X = S or Se) where the donor atoms are connected by a six-membered ring while type *III* set contains complexes 11 and 12 with the same core as in type *II* but the donor atoms are connected by an eight-membered chelate ring (see Scheme 1 and Figure 1).

All twelve complexes have oxygen/ sulphur/selenium donors exhibiting a distorted tetrahedral geometry. Some selected structural parameters are noted in Table 1; elongation of the metal-ligand bond length transpires due to the increase in covalent radii of the donor site as we move from oxygen to selenium. The average Co–O bond length is in the range of 1.940 Å (as found in 2)–2.002 Å (as found in 5). The Co–S bond length ranges from 2.202 Å (in 5) to 2.331 Å (in 1) whereas for Co–Se varies from 2.415 Å (in 6) to 2.444 Å (in 12). The average ∠O–Co–P angles range are found to be 122.3° (in 4) to 128.1° (in 3). The ∠S–Co–P angle however found to be significantly smaller in the range of 97.2° (in 1) to 103.8° (in 11) and the ∠Se–Co–P angle also found to be smaller (99.1° (in 6) to 101.5° (in 12)) because of the difference in the hybridization of the

chalcogenide atomic orbitals. The two chelate rings present in complexes 1–12 are perpendicular to each other and the angle between the two planes formed by the bidentate ligand as depicted in Figure 2 is found to be 75.2° (in 4), 77.4° (in 10) and 89.6° (in 7) and are found to be very similar in other complexes (see Table 1).

The computed *D* and *E/D* and *g*-factors for complexes 1–12 are given in Table 1. Experimentally the magnetic properties are measured only for complexes 1 and 4 and susceptibility data has been fit to obtain *D* value for complex 1 as |11.9| cm⁻¹ (for complex 4 the *D* parameter has not been extracted earlier) where the sign of *D* could not be determined unambiguously.^[9] We attempt to simulate the susceptibility data using PHI^[23] software for both complexes using all the computed parameters and this yield a good fit to the experimental data. This suggests that the computed ZFS parameters are reliable (see Figure S1 in ESI). Furthermore, we have also surveyed earlier reported ZFS parameter of four coordinate Co^{II} to compare and contrast the NEVPT2 estimated *D* and *E/D* values to the experimental values and this list is given in Table S1 in ESI. There are 37 complexes listed and in all cases, the computed values are in very good agreement with experiments offering confidence on the sign and strength *D* and *E/D* estimated here.

Within the types *I–III* proposed, there are some structural similarities and difference, and this is nicely reflected in the estimated ZFS parameters (See Table 1). The type *I* complexes have similar core structure and show maximum negative *D* values while type *II* complexes have the same donor atoms (S or Se) and possess moderate negative *D* values. The type *III* complexes exhibit the largest distortion from *D*_{2d} symmetry among the complexes studied and can be classified as compressed tetrahedron geometry while complexes 1–10 can be considered as an elongated tetrahedron. Due to these distortions present in complexes 11 and 12, they exhibit smaller (positive/negative) *D* value. The ab initio computed *D*_{zz} axis for complexes 1–12 are shown in Figure 1. This axis passes through the highest order (or pseudo) symmetry axis present in the molecule.

We have assigned the point group symmetry of the electronic states of these complexes according to *D*_{2d} symmetry, although none of them possesses a perfect *D*_{2d} point group (see Table S2–S13 in ESI). A

Complexes	Pseudo Symmetry	Dihedral angle [θ _d °]	Avg. Polar angle 2θ [°]	<i>D</i> [cm ⁻¹]	<i>E/D</i>	<i>g</i> _x , <i>g</i> _y , <i>g</i> _z	
type <i>I</i>	1	T _d	86.3	108.2	-19.1 (11.9)*	0.08	2.22, 2.25, 2.46
	2	D _{2d}	85.6	101.2	-46.5	0.04	2.13, 2.18, 2.70
	3	D _{2d}	83.6	99.8	-69.6	0.03	2.10, 2.16, 2.92
	4	D _{2d}	75.2	101.5	-26.8	0.28	2.11, 2.30, 2.52
	5	D _{2d}	86.5	95.5	-117.8	0.02	1.91, 2.02, 3.29
type <i>II</i>	6	D _{2d}	89.2	113.7	-16.8	0.02	2.23, 2.24, 2.44
	7	D _{2d}	89.6	113.5	-12.2	0.01	2.23, 2.24, 2.39
	8	D _{2d}	88.6	112.0	-25.7	0.02	2.23, 2.24, 2.54
	9	D _{2d}	90.0	110.5	-28.8	0.00	2.21, 2.21, 2.55
	10	D _{2d} or C _{2v}	77.4	111.5	18.1	0.22	2.40, 2.31, 2.15
type <i>III</i>	11	C _{2v}	83.6	116.0	10.8	0.25	2.35, 2.29, 2.20
	12	C _{2v}	88.8	113.6	-9.7	0.20	2.24, 2.29, 2.38

* experimental *D* reported from fitting the susceptibility data.

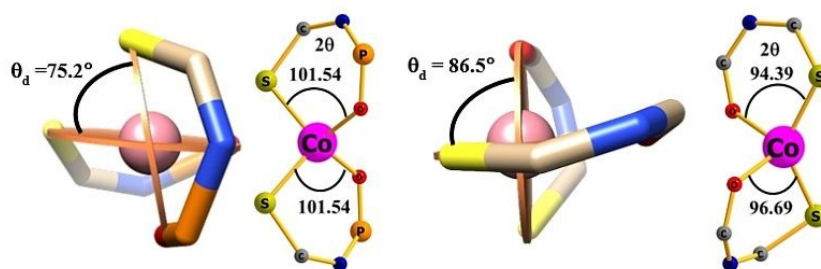


Figure 2. A schematic diagram representing the interplanar dihedral angle (θ_d) and polar angle (2θ) of the complexes 4 (left) and 5 (right). Dihedral angles have been shown in thick stick representation and polar angles have been shown in ball and stick representation of molecules.

perfect D_{2d} symmetric complex will have a dihedral interplanar angle (θ_d) of 90° with a polar angle (2θ) of 90° and degenerate d_{xz} - d_{yz} set of orbitals and minimum d_{xy} - $d_{x^2-y^2}$ orbital energy gap. This type of complexes is ideal for showing enormous negative D value in d^7 electronic configuration.^[7],24] This correlation is valid only when the donor atoms are kept constant, which is O and S donor in the complexes 1–5 as the change in donor atom results in a drastic change in these parameters.^[7a] The estimated D value increases from complexes 1 to 5. The NEVPT2 computed ligand field d-orbital splitting diagram of type I complexes has been shown in Figure 3. It is noticeable

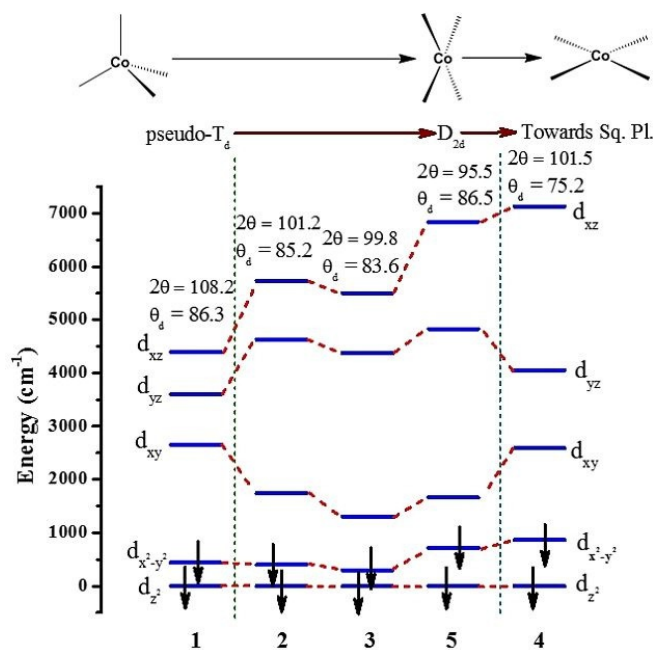


Figure 3. NEVPT2-LFT splitting of the d-orbitals of complexes 1–5. Showing only the spin-down β -orbitals and their corresponding energies.

from Figure 3, that the splitting pattern changes from distorted tetrahedral C_{2v} geometry in complex 1 to pseudo D_{2d} geometry in complex 5. Complex 4 deviates from D_{2d} as the interplanar dihedral angle here is 75° making it closer to rhombic symmetry, and the 2θ value is 101.5° adopting distorted square planar arrangement. It is to be noted here that we have not considered another important torsional angle parameter of X-Co-X-Y (ω) as the ligands here are bidentate in nature and therefore ω does not vary much across the structures. It is observed that the axial and rhombic anisotropies (D and E/D) strongly depend on angle 2θ and dihedral angle θ_d .^[5,7c,g,i,25]

Furthermore, wavefunction analysis reveals a multi-configurational character of the ground state wavefunction for complex 1 and this is due to weaker ligand field splitting compared to complexes 2–5 that allows the ground state to mix with the other excited states. By looking at the d-orbital splitting pattern, one can easily point out the large and small D values estimated are correlated to the $d_{x^2-y^2}$ - d_{xy} energy gap or ${}^4B_1 \rightarrow {}^4B_2$ transition. This is found to be the first excited state for all complexes studied and found to control the D value in all cases by

contributing a large negative D to the overall ZFS parameter (see Table S2–S6 in ESI). Thus except in complex 4, this ${}^4B_1 \rightarrow {}^4B_2$ gap decreases in the order 2844, 1567, 1050 and 418 cm^{-1} and their contribution towards D increases in the order as -41 , -67 , -92 and -138 cm^{-1} for complexes 1–5, respectively. There are other minor positive contributions from the coupling of 4B_1 state with 4E_x state and 4E_y state which mainly arises due to $d_z^2/d_{x^2-y^2} \rightarrow d_{yz}$ and or $d_{z^2}/d_{x^2-y^2} \rightarrow d_{xz}$ electronic excitation. A perfect D_{2d} symmetry will have degenerate 4E_x and 4E_y level, however, if the geometry deviates from this symmetry, the corresponding E level splits. A large rhombic ZFS, i.e., E/D is present (0.28) in complex 4, which arises due to the significant deviation observed in the planar angle indicating a significant departure from ideal D_{2d} symmetry. The same is also causing the D value to be small compared to other complexes.

Type II and III (complexes 6–12) are homoleptic complexes where the coordination around the Co^{II} are either S or Se. However, complexes 6–10 possess pseudo D_{2d} geometry with six-membered ring ligand chelation similar to that of complexes 1–5. The NEVPT2-LFT (ligand field theory) computed d-orbital diagram for complexes 6, 7 and 10 are shown in Figure 4 (see below). A noticeable decrease in energy level splitting can be observed on these three complexes compared to complexes 1–5, as donor strength decreases in the order $\text{CoO}_2\text{S}_2 > \text{CoS}_4 > \text{CoSe}_4$. Additionally, within these three complexes, S has a stronger ligand field than Se, therefore the $\Delta E(d_{x^2-y^2}, d_{xy})$ is larger in complex 7 compared to that 6 leading to smaller D value in 7.

The θ_d is close to 90° in complexes 6–9 which keep the E/D as minimum as possible, but sizeable 2θ of $>110^\circ$ found in five complexes lowers the magnitude of D value compared to complexes 1–5. In contrast to complexes 6–9, complex 10 has smaller θ_d value (77.4°) because of which the sign of D changes to positive and this result is consistent with the prediction made earlier.^[25] A smaller θ_d alters the splitting pattern

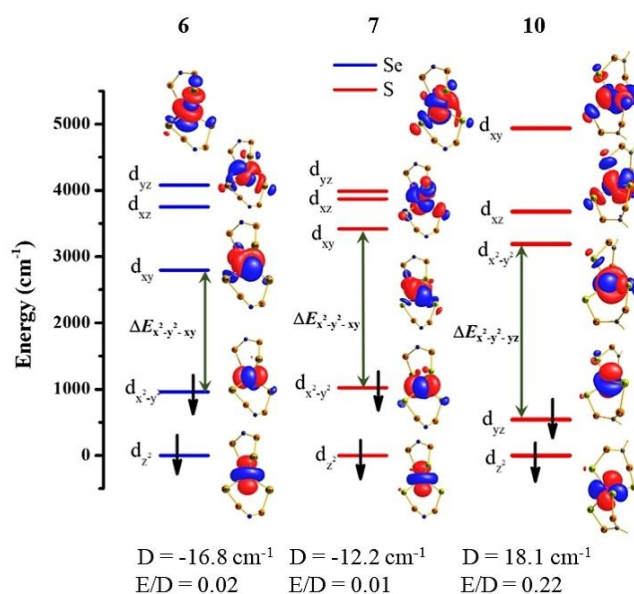


Figure 4. NEVPT2-LFT d-orbital diagram of complexes 6, 7 and 10 along with their ZFS parameters written below.

and pushes it towards square planar geometry. These structural parameters destabilise the $d_{x^2-y^2}$ orbital significantly while d_{yz} orbital is stabilised. This alters the whole splitting pattern as shown in Figure 4 (splitting pattern of **8** and **9** are considered to be similar to **6** and **7**). Unlike in complexes **6–9** where the major contributing transition for the negative D value is $d_{x^2-y^2} \rightarrow d_{xy}$ which has same M_L level.^[26] However, alteration in the splitting pattern in complex **10** led to a dominant contribution to D arise from $d_{yz} \rightarrow d_{x^2-y^2}$ transition and hence the sign of D is positive (different M_L level transition).

Furthermore, to analyse the effect of bulkier phenyl groups at the second coordination sphere atom, complexes which are analogues to **6** and **7** are identified. Complexes **8** and **9** are thus similar to complexes **6** and **7**, respectively, except for the substitution of phenyl groups by isopropyl groups. The calculated ZFS parameters of complex **8** are $D = -25.7 \text{ cm}^{-1}$ with an E/D of 0.02 where the θ_d is 88.6° and the 2θ angle is 112.02° . For complex **9**, the D value is estimated to be -28.8 cm^{-1} with an E/D of 0.00. The θ_d is 90° and 2θ value is 110.5° . The θ_d value is almost similar for **6–9**; however, there are some variations in the 2θ values. In addition to this effect, there is also the electronic effects of the substituents that are expected to influence the donor capabilities. To assess which factor has a dominant control on the magnitude of D value, we have modelled complexes **6** and **7** where the peripheral phenyl groups are substituted by methyl group (See Figure S3 in ESI) and these models (**6a** and **7a**) yield the D value of -17.5 cm^{-1} , -13.4 cm^{-1} with the E/D value of 0.03 and 0.02 respectively. These values have only minor perturbations compared to complexes **6** and **7** and suggest that the electronic effects have lesser influence over the structural factors. We would like to note here that the only difference between complex **6** vs. **8** and **7** vs. **9** are 1.5° and 3° difference in 2θ values, respectively. This small change in the 2θ values enhances the magnitude of D values significantly in complexes **7** and **9** unveiling the influential role of the polar angles in controlling the magnitude of D values in this set of complexes.

Moving to the type *III*, complexes **11** and **12** have 8-membered chelate rings compared to 6-membered rings in previous examples. These two complexes have the largest deviation of both 2θ angle and θ_d value from 90° (see Table 1). As the θ_d values are significantly different here (only other complex to have such large θ_d value is complex **10**), this is reflected in the computed D_{zz} orientation of the molecules (see Figure 2) with their deviation from the proper C_2 axis of D_{2d} symmetry. The drastic change in the D_{zz} orientation also associated with the compressed tetrahedron geometry that is observed for these two complexes. The d-orbital splitting of the last two complexes has been shown in Figure S4 in ESI. Among the two complexes, complex **11** found to show the strongest deviation in both θ_d and 2θ values and this lead to a very large E/D of 0.25 with a positive D . Also at lower θ_d (approaching 60°) and higher polar angle (approaching 120°) the geometry departs from ideal D_{2d} symmetry and approaches square planar or compressed tetrahedron arrangement accompanied by a large E/D value which switches the sign of D as reported earlier by us.^[25] Complex **12**, on the other hand, has a lesser deviation

from 90° for both θ_d and 2θ values compare to complex **11**. Furthermore, the d-orbital splitting also decreases here due to the presence of Se as donor atoms compared to S (see Figure S4 in ESI). These combined effect yields a negative D in complex **12** (-9.7 cm^{-1}) with a significant E/D value (0.2). Additionally, for all the complexes **10–12**, calculations yield significant mixing of the ground state wavefunction with other excited states and to assess this mixing, we have estimated to the ab initio ligand field (AFLT) matrix eigenvalues for the five d-orbitals and these are given in ESI where a strong mixing among the d-orbital is visible. Also, the magnitude of D values in all complexes are strongly correlated to the ground-first excited state gap and this is found to have a linear correlation with the D values with smaller gap yielding a larger negative D value (shown in Figure 5).

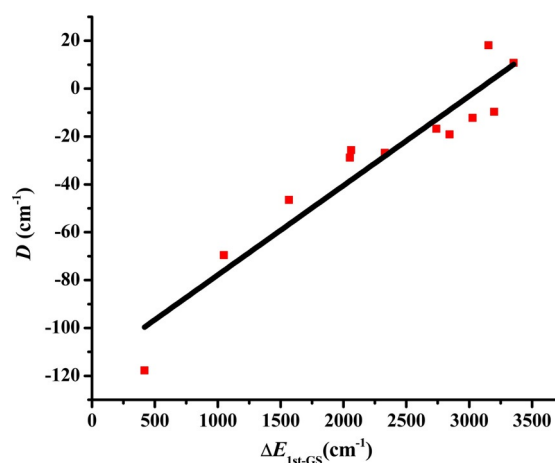


Figure 5. Variation of D values of all the twelve complexes with the energy gap between the ground state and first excited state. Linear fit obtained with a slope 0.04 and intercept -115 and the fit has R-value of 0.90. Red squares indicate the energy gaps obtained from Table S2–S13.

Magneto-structural Maps

In order to understand the relationship between the two structural parameters that are discussed with D and E/D values, we have developed a three-dimensional graph wherein X-ray structural parameters of complexes **1–12** along with its computed D and E/D values are utilized (See Figure 6). From the plots, it is evident that the D value tends to be highly positive at very high 2θ and lower θ_d angles. Rhombic parameter E/D is also high at low θ_d and higher 2θ values. In this regard, E/D is primarily affected by θ_d parameter more than 2θ parameter, hence E/D shows a very high value at lower θ_d irrespective of 2θ values. On the other hand, at the higher θ_d (or close to 90°) and lower 2θ values (or close to 90°), the D becomes as negative as high as -120 cm^{-1} with a minimum E/D value. This trend also supports previously reported experimental results.^[7ij] In case of type *I*, the graph is smooth up to the higher polar angle of 108° , contrary to the entire correlation where there is a downward slope that has been observed at higher dihedral and polar angle $\approx 110^\circ$. This indicates the ability of heavier atom substitution by S/Se with oxygen that switches the sign

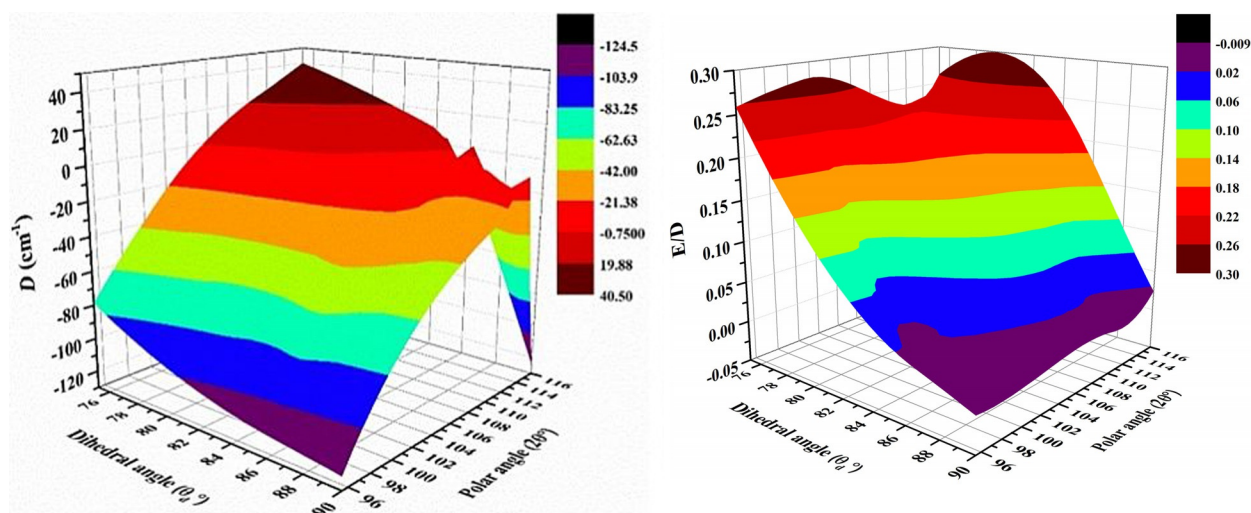


Figure 6. Three dimensional structural correlation map of θ_d vs. 2θ vs. D (left) and θ_d vs. 2θ vs. E/D (right) for complexes 1–12.

of D from positive to negative. From the plot is very clear that D values are primarily controlled by 2θ parameter and E/D values are influenced significantly by θ_d parameter. Thus to have an efficient SIMs, one has to have θ_d value close to 90° and 2θ of less than 96° .

Furthermore, we have also computed the ab initio ligand field parameters (AIFLT) and effective spin-orbit coupling constant (ζ) considering ten quartet roots in all the complexes.^[27] It is established that a decrease in Racah parameter (or the so-called electron-electron repulsion parameter) and SOC constant (ζ) on complexation gives an idea of covalency in the metal-ligand complexes compared to the free ion. Therefore, we have computed both the nephelauxetic reduction in Racah parameter (B) and effective SOC constant for all the complexes 1–12 and compared the values to the free Co^{II} ion value (B_0) and analysed in all the complexes (see Figure 7). A reduction in the B parameter was introduced by calculating $[(1-B/B_0) \times 100\%]$ and reduction in SOC constant was computed as $[(1-\zeta/\zeta_0) \times 100\%]$ for all complexes. It has been noticed that type I complexes are more ionic compared to the type II and type III complexes. It is expected that S and Se donor complexes will have orbitals that are more diffused and hence offer strongly

metal-ligand covalency. The reduction in B and ζ support this point. Additionally, the strong π -donor phenyl rings present in complexes 1, 6–7 and 10–12 in the third coordination sphere shows a stronger nephelauxetic reduction in $B (>9.5\%)$ compared to complexes 2–5 ($<7\%$), 8–9 ($\approx 9\%$) and this indicates that bulky π -donor groups are not suitable for obtaining large negative D value. In case of a nephelauxetic reduction of ζ parameter, complexes 6, 8 and 12 shows largest reduction ($>5.5\%$) as these two complexes contain Se donor atoms in the first coordination sphere and therefore have larger covalency on the Co^{II} -ligand bonding. Here also type I complexes show a smaller reduction in ζ compared to type II and III complexes. A direct correlation between these two parameters and ZFS parameters cannot be drawn as structural parameters have a larger influence in determining the sign and strength of ZFS in four coordinated Co^{II} complexes.

Conclusions

We have studied twelve structurally different $\text{Co}^{\text{II}}\text{X}_4$ complexes using state-of-the-art ab initio calculations, and the following conclusions have been derived from this work.

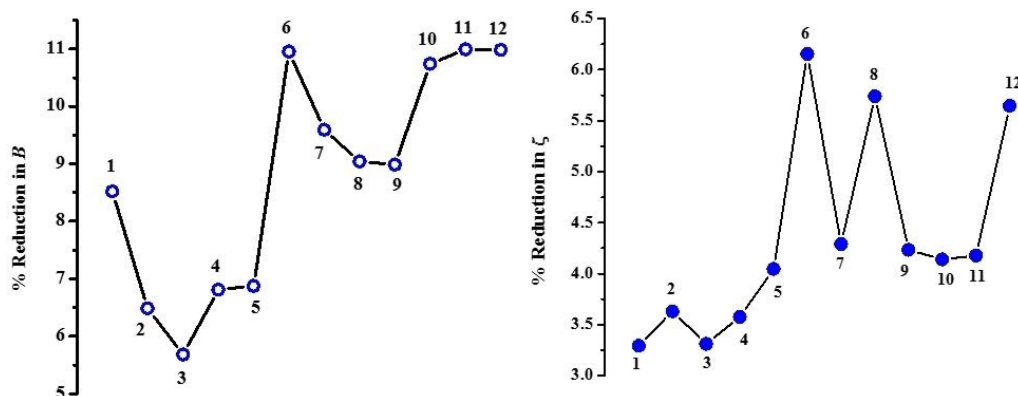


Figure 7. Variation of nephelauxetic reduction of Racah Parameter B (left) and effective spin-orbit coupling constant ζ (right) among the twelve complexes.

- i) The twelve complexes studied have been classified into three types I–III based on the presence of donor atoms O/Se/Sr and the structural arrangement in the first and second coordination sphere. The type I complexes were found to exhibit the largest axial D values among the studied complexes and can be considered as potential single-ion magnets. The variation among the magnitude of D is found to correlate to the structural parameters, particularly the dihedral angle (θ_d) and polar angle (2θ). Among the five complexes studied in this type, complex 5 was found to possess a very large negative D value (-118 cm^{-1}) with a small E/D value and therefore predicted to possess the best SIM characteristics among the complexes tested. Additionally, the $\{\text{CoO}_2\text{S}_2\}$ core tested here has zero nuclear spins on the donor atoms which may help further to reduce the possibility of electro-nuclear coupling mechanism and hence the QTM behaviour.
- ii) Moving to the type II systems where oxygen donor atoms are substituted by S/Se donors was found not to improve the magnitude of ZFS parameters. This suggests that structural parameters are critical in realising a large negative D value than heavier atom substitution. Additionally, substitution on the secondary coordination sphere atoms was found to also influence the magnitude of D . For example, larger or bulkier phenyl groups present in complexes 1 and 6–7 and 10–12 lead to structural distortions. These distortions result in a significant departure from D_{2d} geometry for these molecules and hence smaller D values. Support for these conclusions are derived from complexes 8 and 9 which are structural analogues to complexes 6 and 7, except the bulky phenyl groups are replaced by isopropyl groups. The enhancement in the D value in these two structures are also accompanied by an alteration in the θ_d and 2θ values.
- iii) For type III complexes which have similar first coordination sphere to type II systems, however, a different second coordination sphere arrangement is present. This lead to a large variation in both the θ_d and 2θ values leading to positive and negative D with a very large E/D value. A magneto-structural map that is developed using all the twelve complexes clearly reveals that to obtain large negative D , one has to have larger θ_d and smaller 2θ parameters. Between these two parameters, 2θ was found to control the sign and magnitude of D significantly while θ_d was found to play a critical role in determining E/D values. To have a large negative D and close to zero E/D value, one has to strike a balance between these two parameters, and θ_d close to 90° and 2θ less than 95° are predicted to yield excellent SIM behaviour.

To this end, we have studied twelve Co^{II} four coordinate complexes, which show D values in the range of $+19 \text{ cm}^{-1}$ to -118 cm^{-1} , despite possessing very similar structural motifs. This offers the chemist a viable playground in the design and development of novel single-ion magnets.

Acknowledgements

A.S. would like to acknowledge CSIR for SRF fellowship. G.R. would like to thank SERB (CRG/2018/000430) and UGC-UKEIRI (Grant number 184-4/2018(IC)) for funding.

Conflict of interest

The authors declare no conflict of interest.

Keywords: ab initio calculations • magneto-structural correlation • NEVPT2 methods • single-ion magnets • zero-field splitting

- [1] a) D. Gatteschi, R. Sessoli, J. Villain, *Molecular nanomagnets*, Vol. 5, Oxford University Press on Demand, Oxford, **2006**; b) R. Winpenny, G. Aromí, *Single-molecule magnets and related phenomena*, Springer, Amsterdam, **2006**.
- [2] a) C. A. P. Goodwin, F. Ortu, D. Reta, N. F. Chilton, D. P. Mills, *Nature* **2017**, *548*, 439–442; b) F. S. Guo, B. M. Day, Y. C. Chen, M. L. Tong, A. Mansikkamäki, R. A. Layfield, *Angew. Chem. Int. Ed.* **2017**, *56*, 11445–11449; *Angew. Chem.* **2017**, *129*, 11603–11607; c) F.-S. Guo, B. M. Day, Y.-C. Chen, M.-L. Tong, A. Mansikkamäki, R. A. Layfield, *Science* **2018**, *362*, 1400–1403.
- [3] a) J. M. Zadrozny, D. J. Xiao, M. Atanasov, G. J. Long, F. Grandjean, F. Neese, J. R. Long, *Nat. Chem.* **2013**, *5*, 577–581; b) G. A. Craig, A. Sarkar, C. H. Woodall, M. A. Hay, K. E. R. Marriott, K. V. Kamenev, S. A. Moggach, E. K. Brechin, S. Parsons, G. Rajaraman, M. Murrie, *Chem. Sci.* **2018**, *9*, 1551–1559; c) P. C. Bunting, M. Atanasov, E. Damgaard-Møller, M. Perfetti, I. Crassee, M. Orlita, J. Overgaard, J. Van Slageren, F. Neese, J. R. Long, *Science* **2018**, *362*, eaat7319; d) X.-N. Yao, J.-Z. Du, Y.-Q. Zhang, X.-B. Leng, M.-W. Yang, S.-D. Jiang, Z.-X. Wang, Z.-W. Ouyang, L. Deng, B.-W. Wang, S. Gao, *J. Am. Chem. Soc.* **2017**, *139*, 373–380.
- [4] M. Mannini, F. Pineider, P. Sainctavit, C. Danieli, E. Otero, C. Sciancalepore, A. M. Talarico, M. A. Arrio, A. Cornia, D. Gatteschi, R. Sessoli, *Nat. Mater.* **2009**, *8*, 194–197.
- [5] S. Vaidya, S. Tewary, S. K. Singh, S. K. Langley, K. S. Murray, Y. Lan, W. Wernsdorfer, G. Rajaraman, M. Shanmugam, *Inorg. Chem.* **2016**, *55*, 9564–9578.
- [6] a) F. Shao, B. Cahier, E. Riviere, R. Guillot, N. Guihery, V. E. Campbell, T. Mallah, *Inorg. Chem.* **2017**, *56*, 1104–1111; b) M. A. Hay, A. Sarkar, G. A. Craig, L. Bhaskaran, J. Nehrkorn, M. Ozerov, K. E. R. Marriott, C. Wilson, G. Rajaraman, S. Hill, M. Murrie, *Chem. Sci.* **2019**, *10*, 6354–6361.
- [7] a) S. Vaidya, A. Upadhyay, S. K. Singh, T. Gupta, S. Tewary, S. K. Langley, J. P. Walsh, K. S. Murray, G. Rajaraman, M. Shanmugam, *Chem. Commun.* **2015**, *51*, 3739–3742; b) S. Vaidya, S. K. Singh, P. Shukla, K. Ansari, G. Rajaraman, M. Shanmugam, *Chem. Eur. J.* **2017**, *23*, 9546–9559; c) K. Chattopadhyay, M. J. H. Ojea, A. Sarkar, M. Murrie, G. Rajaraman, D. Ray, *Inorg. Chem.* **2018**, *57*, 13176–13187; d) S. Vaidya, P. Shukla, S. Tripathi, E. Riviere, T. Mallah, G. Rajaraman, M. Shanmugam, *Inorg. Chem.* **2018**, *57*, 3371–3386; e) S. Tripathi, S. Vaidya, K. U. Ansari, N. Ahmed, E. Riviere, L. Spillecke, C. Koo, R. d. Klingeler, T. Mallah, G. Rajaraman, *Inorg. Chem.* **2019**, *58*, 9085–9100; f) X.-N. Yao, M.-W. Yang, J. Xiong, J.-J. Liu, C. Gao, Y.-S. Meng, S.-D. Jiang, B.-W. Wang, S. Gao, *Inorg. Chem. Front.* **2017**, *4*, 701–705; g) E. A. Suturina, D. Maganas, E. Bill, M. Atanasov, F. Neese, *Inorg. Chem.* **2015**, *54*, 9948–9961; h) A. K. Mondal, M. Sundararajan, S. Konar, *Dalton Trans.* **2018**, *47*, 3745–3754; i) M. S. Fataftah, S. C. Coste, B. Vlasisavljevich, J. M. Zadrozny, D. E. Freedman, *Chem. Sci.* **2016**, *7*, 6160–6166; j) Y. Rechkemmer, F. D. Breitgoff, M. van der Meer, M. Atanasov, M. Haki, M. Orlita, P. Neugebauer, F. Neese, B. Sarkar, J. van Slageren, *Nat. Commun.* **2016**, *7*, 10467.
- [8] a) J. M. Zadrozny, J. R. Long, *J. Am. Chem. Soc.* **2011**, *133*, 20732–20734; b) J. M. Zadrozny, J. Telsler, J. R. Long, *Polyhedron* **2013**, *64*, 209–217.
- [9] M. C. Aragoni, M. Arca, M. B. Carrea, A. Garau, F. A. Devillanova, F. Isaia, V. Lippolis, G. L. Abbati, F. Demartin, C. Silvestru, *Eur. J. Inorg. Chem.* **2007**, 4607–4614.

- [10] D. A. Safin, P. Mlynarz, F. E. Hahn, M. G. Babashkina, F. D. Sokolov, N. G. Zabiroy, J. Galezowska, H. Kozlowski, *Z. Anorg. Allg. Chem.* **2007**, *633*, 1472–1479.
- [11] F. D. Sokolov, N. G. Zabiroy, L. N. Yamaliev, V. G. Shtyrlin, R. R. Garipov, V. V. Brusko, A. Y. Verat, S. V. Baranov, P. Mlynarz, T. Glowiak, *Inorg. Chim. Acta* **2006**, *359*, 2087–2096.
- [12] D. A. Safin, P. Mlynarz, F. D. Sokolov, M. Kubiak, F. E. Hahn, M. G. Babashkina, N. G. Zabiroy, J. Galezowska, H. Kozlowski, *Z. Anorg. Allg. Chem.* **2007**, *633*, 2089–2096.
- [13] K. Ramasamy, M. A. Malik, J. Raftery, F. Tuna, P. O'Brien, *Chem. Mater.* **2010**, *22*, 4919–4930.
- [14] J. Novosad, M. Necas, J. Marek, P. Veltsistas, C. Papadimitriou, I. Haiduc, M. Watanabe, J. D. Woollins, *Inorg. Chim. Acta* **1999**, *290*, 256–260.
- [15] M. C. Aragoni, M. Arca, A. Garau, F. Isaia, V. Lippolis, G. L. Abbati, A. C. Fabretti, *Z. Anorg. Allg. Chem.* **2000**, *626*, 1454–1459.
- [16] L. M. Gilby, B. Piggott, *Polyhedron* **1999**, *18*, 1077–1082.
- [17] H. Heuclin, T. Cantat, X. F. Le Goff, P. Le Floch, N. Mezailles, *Eur. J. Inorg. Chem.* **2011**, 2540–2546.
- [18] J. Ellermann, J. Sutter, F. A. Knoch, M. Moll, *Chem. Ber.* **1994**, *127*, 1015–1020.
- [19] F. Neese, *WIREs* **2018**, *8*, e1327.
- [20] C. van Wüllen, *J. Chem. Phys.* **1998**, *109*, 392–399.
- [21] F. Weigend, R. Ahlrichs, *Phys. Chem. Chem. Phys.* **2005**, *7*, 3297–3305.
- [22] R. Maurice, R. Bastardis, C. de Graaf, N. Suaud, T. Mallah, N. Guihery, *J. Chem. Theory Comput.* **2009**, *5*, 2977–2984.
- [23] N. F. Chilton, R. P. Anderson, L. D. Turner, A. Soncini, K. S. Murray, *J. Comput. Chem.* **2013**, *34*, 1164–1175.
- [24] M. S. Fataftah, J. M. Zadrozny, D. M. Rogers, D. E. Freedman, *Inorg. Chem.* **2014**, *53*, 10716–10721.
- [25] A. Sarkar, G. Velmurugan, T. Rajeshkumar, G. Rajaraman, *Dalton Trans.* **2018**, *47*, 9980–9984.
- [26] S. Gomez-Coca, E. Cremades, N. Aliaga-Alcalde, E. Ruiz, *J. Am. Chem. Soc.* **2013**, *135*, 7010–7018.
- [27] S. K. Singh, J. Eng, M. Atanasov, F. Neese, *Coord. Chem. Rev.* **2017**, *344*, 2–25.

Manuscript received: August 14, 2019

Revised manuscript received: September 4, 2019

Accepted manuscript online: September 6, 2019

Version of record online: September 20, 2019
